Feedback Control of an Underactuated Planar Bipedal Robot with Impulsive Foot Action

Jun Ho Choi and J. W. Grizzle

Abstract

A planar underactuated bipedal robot with an impulsive foot model is considered. The analysis extends previous work on a model with unactuated point feet of Westervelt *et al.*[1] to include the actuator model of Kuo[2]. The impulsive actuator at each leg end is active only during the double support phase, which results in the model being identical to the model with unactuated point feet for the single support phase. However, the impulsive foot actuation results in a different model for the double support map. Conditions for the existence of a hybrid zero dynamics for the robot with foot actuation are studied. A feedback design method is proposed that integrates actuation in the single and double support phases. A stability analysis is performed using a Poincaré return map. As in Kuo's model[2], a more efficient gait is demonstrated with an impulsive foot action.

I. INTRODUCTION

During walking, some of the mechanical energy of a robot is lost from impacts between the swing leg and the ground. The energy lost during the impacts needs to be replaced in order to have a periodic motion. Although it is possible to provide the energy by actuators at the joints during single support phase, it was suggested that a more energy-efficient gait could be achieved with impulsive force applied at the stance foot[2]. In this paper, a planar bipedal robot with impulsive foot action is studied. This is an approximation of the toe-off action observed in double support phases of human walking[3]. The model studied in this paper is an extension of the model with unactuated point feet by Westervelt *et al.*[1] and the 2-link model with impulsive foot action by Kuo[2].

Robots with various types of foot action have been studied in the literature. McGeer analyzed a robot that had arc-shaped unactuated feet[4], which had no foot action. Linde investigated a 2-link robot that had a variable spring and damper at

Jun Ho Choi and J. W. Grizzle are with the Department of Electrical Engineering and Computer Science, University of Michigan, Ann Arbor, Michigan 48109-2122, USA {junhoc, grizzle}@umich.edu

each leg with arc-shaped unactuated feet[5]. Yi studied a robot that had a passive ankle, specifically, the ankle joints were connected with springs[6]. A robot with point feet that assumed "ankle-actuation" during the single support phase was studied by Asano *et al.*[7] Many papers in the literature have considered actuated feet with nontrivial length, with the sole of the stance foot remaining flat on the ground during the single-support phase[8–10]. Since keeping the support sole on the ground limits the motion of the robot, it has been suggested to allow the foot to roll with respect to the stance toe[11,12].

Grizzle *et al.*, for planar robot models with one degree of underactuation in single support, introduced a feedback method whereby existence and stability of periodic orbits could be determined by a one-dimensional map[13]. A key aspect of the analysis uses the notion of virtual constraints, that is, holonomic constraints that are asymptotically imposed on the robot's motion via feedback control. Westervelt *et al.* introduced the notion of the hybrid zero dynamics, which transformed the method of virtual constraints into a practical design method, capable of treating N-link planar bipedal robots with point feet and one degree of underactuation[1]. Extensive experiments have been reported[14,15].

Although impulsive foot action is not necessary for stable walking, as shown by McGeer[4], Grizzle *et al.*[13], and Westervelt *et al.*[1], the possibility of more efficient walking with impulsive foot action was shown by Hardt *et al.*[16] and Kuo[2]. Hardt *et al.* simulated a robot with impulsive foot action, where the impulsive foot force was applied at the beginning of the single support phase[16]. In their simulation, a 5-link model with impulsive foot actuation showed more energy efficient walking than a robot without the foot action. A 2-link model with impulsive point feet has been studied by Kuo, who investigated the energetics of powered locomotion[2]. The robot was planar and consisted of a massive hip and two rigid massless legs. An impulsive foot actuator was attached at the end of the stance leg. The impulsive toe-off actuation was applied just *before* heel strike. Using this model, it was shown that applying toe-off force is more energy efficient than using hip torque alone.

In this paper, the impulsive foot actuator is assumed to be active during the double support phase. This results in the identical model of Westervelt *et al.*[1] during the single support phase. However, due to the impulsive foot actuator during the double support phase, the double support map becomes a function of not only the states before the double support phase but also the foot force during the double support phase. The notion of the hybrid zero dynamics is extended to accommodate the presence of the foot force. A class of foot force control laws is introduced to create the invariance of the zero dynamics. The Poincaré map is also used to analyze the stability of the robot's motion.

In Section II, the model of the robot with impulsive foot action is presented. In Section III, the existence of the hybrid zero dynamics is addressed. In Section IV, the stability of the robot is proved using a Poincaré return map. In Section V, the output function for the hybrid zero dynamics is parameterized using Bézier polynomials for optimization. In Section

VI, simulation results for a robot in Chevallereau *et al.*[17] with the addition of impulsive foot action are presented. The paper is concluded in Section VII.

II. ROBOT MODEL WITH IMPULSIVE FEET

The model considered in this paper is extended from the model with unactuated point feet[1] by adding an impulsive actuator at each foot. The robot is assumed to be planar, bipedal, and have N rigid links with mass. Each connection of the links is in the form of an actuated revolute joint. Since the robot has point feet, there is no torque applied between the leg and the ground. A typical robot model with 5-link is shown in Fig. 1. Walking is assumed to consist of two phases, which are single support and double support. The double support phase is assumed to have a foot actuation subphase and an impact subphase, see Fig. 2. It is assumed that the impulsive actuator at the stance foot is activated only in the foot actuation subphase, and when active, applies a unilateral force along the direction of the link in contact with the ground. Therefore, during the single support phase, the model is identical to a robot with unactuated point feet. The detailed assumptions for the single support phase are based on Westervelt *et al.*[1] and are listed in Appendix A for the convenience of the readers.

During the single support phase, the robot is underactuated since the impulsive foot actuator at the stance foot is not activated. Therefore, the model for the single support phase is identical to the one with unactuated point feet, which is given as

$$D(q)\ddot{q} + C(q,\dot{q})\dot{q} + G(q) = B\Gamma, \tag{1}$$

where $q = (q_1, \cdots, q_N)^T \in \mathcal{Q}$, $\mathcal{Q}$ is a simply connected subset of $[0, 2\pi)^N$, q are the configuration variables, $\dot{q}$ are the velocities, and $\Gamma = (\Gamma_1, \cdots, \Gamma_{N-1})^T$ are the input torques applied at the joints. Let $x = (q^T, \dot{q}^T)^T \in T\mathcal{Q}$. Then the dynamic equation in state-space form is given by $\dot{x} = f(x) + g(x)\Gamma$.

Property 1: Consider hypothesis RH5 in Appendix A (that is, the coordinates of the robot consist of $N-1$ relative angles, $q_1, \cdots, q_{N-1}$, and one absolute angle q_N,) and assume furthermore that q_N is measured in the counterclockwise direction. Then the angular momentum of the robot about the stance leg end during the single support phase is $\sigma = d_N(q)\dot{q}$, where $d_N(q)$ is the last row of D in (1).

Proof: See Appendix B. ■

In general, the angular momentum of the robot and $d_N(q)\dot{q}$ are related as $d_N(q)\dot{q} = \pm\sigma$ depending on the direction of q_N.

During the double support phase, the foot actuation subphase and the impact subphase occur successively within an infinitesimally small time interval. The foot actuation subphase is when the actuator at the stance foot is active. It applies an impulsive force to the robot in the direction of the stance tibia, causing a discontinuous change in the velocity states. The impact subphase is when the swing leg touches the ground after the foot actuation. The impact also causes an impulsive reaction force to the robot, which results in another discontinuous change in the velocity states. In both cases, the position states remain continuous. The overall double support phase becomes an algebraic mapping that maps the states just before the foot actuation to the states right after the impact. The double support map therefore depends not only on the states before the foot actuation, but also on the applied foot force.

Based on Kuo[2], the necessary hypotheses for the impulsive foot action are :

IFH1) The double support phase lasts for an infinitesimally small period of time;

IFH2) The double support phase has two sequential subphases, namely, the foot actuation subphase and the impact subphase;

IFH3) The foot actuation subphase occurs just before the impact subphase, with the time interval between the two subphases being infinitesimally small;

IFH4) There is an impulsive foot actuator at the end of each tibia, which is activated only during the foot actuation subphase;

IFH5) Impulsive foot force causes discontinuous changes in the velocity states but the position states remain continuous;

IFH6) The foot force is applied along the stance tibia, that is, the direction of the force is the same as the stance tibia;

IFH7) The applied foot force is unilateral, in other words, it cannot pull the robot down to the ground.

To describe the double support phase, it is necessary to use an N+2 DOF model (e.g. N DOF for the joints and 2 DOF for the position of the stance end). Adding Cartesian coordinates, (p_1^h, p_1^v), to the end of the stance leg gives $q_e = (q^T, p_1^h, p_1^v)^T$ and $\dot{q}_e = (\dot{q}^T, \dot{p}_1^h, \dot{p}_1^v)^T$, see Fig. 3. Let ϕ_1 and ϕ_2 be the angles of the foot actuation force and the impulsive ground reaction force, computed with respect to the vertical, respectively. Using the method of Lagrange, the dynamics for the double support phase are obtained as follows:

$$D_e(q_e)\ddot{q}_e + C_e(q_e, \dot{q}_e)\dot{q}_e + G_e(q_e) = B_e\Gamma + E_e^1\delta F_1 + E_e^2\delta F_2, \tag{2}$$

where $\Upsilon_1(q_e)$ and $\Upsilon_2(q_e)$ denote the Cartesian coordinates of the stance leg end and swing leg end, respectively, $E_e^1 = \left(\frac{\partial \Upsilon_1(q_e)}{\partial q_e}\right)^T$, $E_e^2 = \left(\frac{\partial \Upsilon_2(q_e)}{\partial q_e}\right)^T$, and δF_1 and δF_2 denote the impulsive foot force and the impulsive ground reaction force, respectively.

During the foot actuation subphase, $F_1 = \mathcal{T}\delta F_f$ and $\delta F_2 = 0$, where

$$\mathcal{T} = \begin{bmatrix} \sin\phi_1 \\ \cos\phi_1 \end{bmatrix}. \tag{3}$$

Let q_e^1 be the state vector for the foot actuation subphase. Then, following the procedure in Grizzle *et al.* [13], (2) becomes

$$D_e(\dot{q}_e^{1+} - \dot{q}_e^{1-}) = E_e^1 \mathcal{T} F_f, \tag{4}$$

where $F_f = \int \delta F_f \, dt$, $\dot{q}_e^{1+}$ is the velocity just after the foot actuation and $\dot{q}_e^{1-}$ is the velocity just before the foot actuation. Since the stance foot acts as a pivot before the double support phase, $\dot{q}_e^{1-} = (\dot{q}^{-T}, 0, 0)^T$.

Property 2: Under hypotheses RH5 and GH2 (that is, the stance foot acts as a pivot in single support) in Appendix A, $d_N(q^-)\dot{q}^- = d_{e,N}(q_e^-)\dot{q}_e^-$, where $d_{e,N}(q_e)$ is the Nth row of D_e in (2).

Proof: See Appendix B. ■

Property 3: Assume the hypothesis RH5 in Appendix A. Then $d_{e,N}(q_e^{1-})\dot{q}_e^{1-} = d_{e,N}(q_e^{1+})\dot{q}_e^{1+}$ in the coordinates $q_e^1 = (q_1, \cdots, q_N, p_1^h, p_1^v)$, where q_e^{1-}, $\dot{q}_e^{1-}$ are the states before the foot actuation and q_e^{1+}, $\dot{q}_e^{1+}$ are the states after the foot actuation.

Proof: See Appendix B ■

Properties 2 and 3 imply that the angular momentum about the stance leg end is conserved even with impulsive foot actuation. The change in linear momentum is studied next.

Property 4: Let $\vec{P}_c^+, \vec{P}_c^-$ be the linear momentum of the robot after and before foot actuation. Then $\vec{P}_c^+ - \vec{P}_c^- = \mathcal{T} F_f$.

Proof: See Appendix B. ■

Since D_e in (4) is positive definite, it is always possible to calculate the velocity states after the foot actuation. The velocity states after the foot actuation are given as

$$\dot{q}_e^{1+} = \dot{q}_e^{1-} + (D_e)^{-1} E_e^1 \mathcal{T} F_f. \tag{5}$$

Right after the foot force is applied to the stance leg, the swing leg makes contact with the ground, which is the impact subphase. During the impact subphase, $\delta F_1 = 0$ and $\delta F_2 = \begin{bmatrix} \delta F_2^T \\ \delta F_2^N \end{bmatrix}$, where δF_2^T and δF_2^N denote the tangential and normal components of the impulsive reaction force. Following the procedure in Grizzle *et al.* [13] again, (2) becomes

$$D_e(\dot{q}_e^{2+} - \dot{q}_e^{2-}) = E_e^2 F_2, \tag{6}$$

where $F_2 = \int \delta F_2 \, dt$, $\dot{q}_e^{2+}$ is the velocity just after the impact, and $\dot{q}_e^{2-}$ is the velocity just before the impact.

Property 5: Under hypotheses RH5 and GH2 in Appendix A, $d_N(q^{2+})\dot{q}^{2+} = d_{e,N}(q_e^{2-})\dot{q}_e^{2-}$.

Proof: The proof is analogous to the proof of property 2. ■

Property 6: Assume the hypothesis RH5 in Appendix A. Then in the coordinate $q_e^2 = (q_1, \cdots, q_N, p_2^h, p_2^v)$, $d_{e,N}(q_e^{2-})\dot{q}_e^{2-} = d_{e,N}(q_e^{2+})\dot{q}_e^{2+}$, where q_e^{2-}, $\dot{q}_e^{2-}$ are the states before impact and q_e^{2+}, $\dot{q}_e^{2+}$ are the states after impact.

Proof: The proof is analogous to the proof of property 3. ■

Properties 5 and 6 imply the angular momentum about the swing leg end is conserved during the impact of the swing leg end.

By IH1, the swing leg does not slip during the impact. Hence,

$$\frac{\partial \Upsilon_2}{\partial q_e}\dot{q}_e^{2+} = (E_e^2)^T \dot{q}_e^{2+} = 0. \tag{7}$$

Augmenting (6) and (7) yields

$$\begin{bmatrix} \dot{q}_e^{2+} \\ F_2 \end{bmatrix} = \Pi \begin{bmatrix} D_e \dot{q}_e^{2-} \\ 0 \end{bmatrix}, \tag{8}$$

where Π is defined as

$$\Pi = \begin{bmatrix} D_e & -E_e^2 \\ (E_e^2)^T & 0 \end{bmatrix}^{-1}. \tag{9}$$

By assumption IFH3, there is an infinitesimally small time interval between the foot actuation and the impact, which implies that $q_e^{1+} = q_e^{2-}$ and $\dot{q}_e^{1+} = \dot{q}_e^{2-}$. Then the velocity states after the impact can be expressed as a function of the states before the foot actuation and the foot force. After the impact, the states need to be relabeled since the swing leg and the stance leg switch their roles for the next step. The overall mapping from the velocity states just before the foot actuation to the velocity states right after the impact is given as follows:

$$\begin{aligned} \dot{q}^+ &= \begin{bmatrix} R & 0 \end{bmatrix} \Pi \begin{bmatrix} D_e \begin{bmatrix} I \\ 0 \end{bmatrix} \\ 0 \end{bmatrix} \dot{q}^- \\ &\quad + \begin{bmatrix} R & 0 \end{bmatrix} \Pi \begin{bmatrix} E_e^1 \mathcal{T} \\ 0 \end{bmatrix} F_f \\ &= \Delta_{\dot{q}2}(q^-)\dot{q}^- + \Delta_{\dot{q}1}(q^-)F_f, \end{aligned} \tag{10}$$

where $\dot{q}^-, \dot{q}^+$ are the velocity states just before the foot action and right after the impact, respectively, and R is a relabeling matrix. Since the position states remain continuous during the double support phase, the position states only need to be

relabeled for the next step, $q^+ = \Delta_q(q^-) = Rq^-$. The double support map is given as

$$x^+ = \begin{bmatrix} q^+ \\ \dot{q}^+ \end{bmatrix} = \begin{bmatrix} \Delta_q q^- \\ \Delta_{\dot{q}2}(q^-)\dot{q}^- + \Delta_{\dot{q}1}(q^-)F_f \end{bmatrix} = \Delta(x^-, F_f). \tag{11}$$

Note that $\Delta_{\dot{q}2} = \Delta_{\dot{q}}$ in Westervelt *et al.*[1] and $\Delta_{\dot{q}1}(q^-)$, $\Delta_{\dot{q}2}(q^-)$ are functions of the position states only.

Following the method in Ye *et al.*[18] gives the overall system description. Let $S = \{x \in T\mathcal{Q} | p_2^h > 0, p_2^v = 0\}$ be a set of states satisfying the conditions for the double support phase, where (p_2^h, p_2^v) represents the Cartesian coordinates of the swing leg end, see Fig. 3. The overall system is given as

$$\begin{cases} \dot{x} = f(x) + g(x)\Gamma, & x^- \notin S, \\ x^+ = \Delta(x^-, F_f), & x^- \in S,\ F_f \in \mathbb{R}^+ \cup \{0\}. \end{cases} \tag{12}$$

Note that the dynamics for the single support phase is identical to the model with unactuated point feet[1] and the double support map becomes identical when the foot force F_f is zero.

III. EXISTENCE OF HYBRID ZERO DYNAMICS

In this section, the existence of a zero dynamics for the hybrid model (12) is studied. This will be a one degree of freedom subdynamic of the full-order model (12) with the property that asymptotically stable orbits of the one degree of freedom subdynamic are asymptotically stabilizable orbits of the full-order model. The systematic design and analysis of a feedback controlled walking motion is much easier on the hybrid zero dynamics. The controller is designed to impose $N-1$ independent holonomic constraints on the robot, and to be invariant under the double support map. With impulsive foot actuation, the hybrid zero dynamics manifold is determined by not only the choice of the output function but also the foot force applied during the double support phase.

Let $y = h(x)$ be a vector of $N-1$ functions satisfying HH1-HH5 of Westervelt *et al.*[1] (see Appendix A), which essentially means that h depends only on the configuration variables during the single support phase, the associated decoupling matrix, $L_g L_f h(x)$, is full rank, and there exists $\theta(q)$ such that $[h^T, \theta(q)]^T$ is a local diffeomorphism on $\tilde{\mathcal{Q}}$, an open set of the configuration space. Then there exists a smooth manifold $Z = \{x \in T\mathcal{Q} | h(x) = 0, L_f h(x) = 0\}$, called the zero dynamics manifold, and $S \cap Z$ is smooth. $S \cap Z$ is one-dimensional if $S \cap Z \neq \emptyset$. Z becomes the state space for the one degree of freedom constrained system, called the zero dynamics. In addition to the hypotheses HH1–HH5, if the

hypothesis RH5 is also satisfied, then the single support phase zero dynamics can be expressed in the form

$$f_{zero}(z): \quad \begin{aligned} \dot{z}_1 &= \kappa_1(z_1) z_2 \qquad (13) \\ \dot{z}_2 &= \kappa_2(z_1) \qquad (14) \end{aligned}$$

where $z_1 = \theta(q)$ and $z_2 = d_N(q)\dot{q}$[1]. By Property 1, z_2 is the angular momentum about the stance foot.

Definition 1: Let Z and $\dot{z} = f_{zero}(z)$ be the zero dynamics manifold of the single support phase and the associated zero dynamics, respectively. Z is a *hybrid zero dynamics manifold* if $\forall z^- \in S \cap Z$, $\exists F_f(z^-) \in \mathbb{R}^+ \cup \{0\}$ such that $\Delta(z^-, F_f(z^-)) \in Z$. In other words, Z is controlled-invariant with respect to the impulsive foot action. The nonlinear system

$$\begin{aligned} \dot{z} &= f_{zero}(z), & z^- &\notin S \cap Z \\ z^+ &= \Delta(z^-, F_f(z^-)), & z^- &\in S \cap Z \end{aligned} \qquad (15)$$

with $z \in Z$ is called the *hybrid zero dynamics* of (12).

Remark 1: By the definition, Z is a hybrid zero dynamic manifold if, and only if, $\forall z^- \in S \cap Z$, $\exists F_f \in \mathbb{R}^+ \cup \{0\}$ such that

$$h \circ \Delta(z^-, F_f) = 0, \qquad (16)$$

$$L_f h \circ \Delta(z^-, F_f) = 0. \qquad (17)$$

□

Let $x(t)$ be a solution of the system (12) for the single support phase with the output $y = h(x)$ being zero. If the trajectory of the solution contains an impact with S then the impact time t_I exists and is finite. Then $x^- := \lim_{t \nearrow t_I} x(t)$ exists and $x^- = (q^-, \dot{q}^-)^T \in S \cap Z$. By HH5, q^- is a unique point in $\tilde{\mathcal{Q}}$ defined as in HH2. Define $\Phi : \mathbb{R} \to S \cap Z$ as

$$\Phi = \begin{bmatrix} \Phi_q \\ \Phi_{\dot{q}} \end{bmatrix}, \qquad (18)$$

where $\Phi_q = q^-$ and

$$\Phi_{\dot{q}}(q^-) = \begin{bmatrix} \frac{\partial h}{\partial q}(q^-) \\ d_N(q^-) \end{bmatrix}^{-1} \begin{bmatrix} 0 \\ 1 \end{bmatrix}, \qquad (19)$$

then Φ is a diffeomorphism[1]. Define $z^- = (\theta^-, \sigma^-) = (\theta(q^-), d_N(q^-)\dot{q}^-)$ then the double support map for the velocity states (10) becomes

$$\begin{aligned} \dot{q}^+ &= \Delta_{\dot{q}1}(q^-) F_f + \Delta_{\dot{q}2}(q^-) \Phi_{\dot{q}}(q^-) \sigma^- \\ &= w_1 F_f + w_2 \sigma^-, \end{aligned} \qquad (20)$$

where $w_1 = \Delta_{\dot{q}1}(q^-)$ and $w_2 = \Delta_{\dot{q}2}(q^-)\Phi_{\dot{q}}(q^-)$. Note that w_1, w_2 are uniquely defined $N \times 1$ vectors.

Let Z be the hybrid zero dynamics manifold. The double support map for θ restricted to Z is given by

$$\theta^+ = \theta \circ \Delta_q(q^-). \tag{21}$$

The double support map of σ restricted to Z is given by

$$\begin{aligned} \sigma^+ &= d_N(q^+)\dot{q}^+ \\ &= d_N(q^+)(\Delta_{\dot{q}2}(q^-)\Phi_{\dot{q}}\sigma^- + \Delta_{\dot{q}1}(q^-)F_f). \end{aligned} \tag{22}$$

Using Properties 1 to 6, it follows that (22) is equivalent to

$$\sigma^+ = \sigma^- + l(Mv_c^{v-} + \cos\phi_1 F_f), \tag{23}$$

where l is the step length, M is the total mass, and v_c^{v-} is the vertical component of the velocity of the center of mass just before the impact.

Theorem 1: Suppose there exists at least one point $\hat{z}^- = (\hat{\theta}^-, \hat{\sigma}^-) \in S \cap Z$ and $\hat{F}_f \in \mathbb{R}^+ \cup \{0\}$ such that $\hat{\sigma}^- \neq 0$, $h \circ \Delta(\hat{z}^-, \hat{F}_f) = 0$, $L_f h \circ \Delta(\hat{z}^-, \hat{F}_f) = 0$, and $\dot{q}^+ \neq 0$. Suppose w_1 and w_2 are not zero, where w_1, w_2 are the vectors defined in (20). Then $\forall z^- = (\theta^-, \sigma^-) \in S \cap Z$, there exists $F_f \in \mathbb{R}^+ \cup \{0\}$ such that $L_f h \circ \Delta(z^-, F_f) = 0$ if, and only if, one of the following is satisfied.

1) The foot force is defined as

$$F_f = \frac{\hat{F}_f}{\hat{\sigma}^-}\sigma^-; \tag{24}$$

2) There exists $\lambda \in \mathbb{R}$ such that

$$D_e \begin{bmatrix} \Phi_{\dot{q}} \\ 0 \end{bmatrix} - \lambda E_e^1 \mathcal{T} \in \mathcal{R}(E_e^2), \tag{25}$$

where $\mathcal{R}(E_e^2)$ is the range space of E_e^2.

Proof: See Appendix C. ■

Although having an output function satisfying the second condition in Theorem 1 enables us to use an arbitrary foot force to achieve the hybrid zero dynamics, designing such an output function is too restrictive. Indeed, the second condition results in w_1 and w_2 being in the null space of $\frac{\partial h(q^+)}{\partial q}$, which is one dimensional. This condition implies that the $\dot{q}^+$ has the same direction for all possible σ^- and F_f, and that the swing leg and the stance leg should have a posture such that the resulting post-impact velocity lies in the direction. Consequently, the foot force during the double support phase is chosen as

$$F_f = r_f \sigma^- \tag{26}$$

with $r_f \in \mathbb{R}^+ \cup \{0\}$, in order to create the hybrid zero dynamics. Then the double support map (22) becomes

$$\begin{aligned} \sigma^+ &= d_N(q^+)(\Delta_{\dot{q}1} r_f + \Delta_{\dot{q}2})\sigma^- \\ &= \delta_z \sigma^-, \end{aligned} \tag{27}$$

where $\delta_z = d_N(q^+)(\Delta_{\dot{q}1} r_f + \Delta_{\dot{q}2})$.

IV. STABILITY ANALYSIS

Using the method of Poincaré section, the stability of the robot restricted to the hybrid zero dynamics manifold is analyzed. Then the stability of the full model is addressed.

By Westervelt *et al.*[1], it was shown that if the robot completes a step within the zero dynamics, then σ is nonzero during the single support phase. Since $\sigma \neq 0$ during the step, $\zeta = \frac{\sigma^2}{2}$ is a valid coordinate transformation. Then, (13) and (14) become

$$d\zeta = \sigma d\sigma = \frac{\kappa_2(\theta)}{\kappa_1(\theta)} d\theta. \tag{28}$$

Let $z^- = (\theta^-, \sigma^-) \in S \cap Z$ and θ^+ be defined as in (21). For $\theta^+ \leq \theta \leq \theta^-$, define

$$V_{zero}(\theta) = -\int_{\theta^+}^{\theta} \frac{\kappa_2(\xi)}{\kappa_1(\xi)}\, d\xi, \tag{29}$$

$$V_{zero}^{max} = \max_{\theta^+ \leq \theta \leq \theta^-} V_{zero}(\theta). \tag{30}$$

If $\delta_z^2 \zeta^- - V_{zero}^{max} > 0$, then (28) can be integrated over a step, which results in

$$\frac{1}{2}(\sigma^-)^2 - \frac{1}{2}(\sigma^+)^2 = \zeta^- - \zeta^+ = -V_{zero}(\theta^-). \tag{31}$$

From (27), $\zeta^+ = \delta_z^2 \zeta^-$. Hence, the reduced Poincaré map in (θ, ζ) coordinates, $\rho(\zeta^-) : S \cap Z \to S \cap Z$, is defined as follows

$$\rho(\zeta^-) = \delta_z^2 \zeta^- - V_{zero}(\theta^-) \tag{32}$$

with domain of definition

$$\mathcal{D} = \{\zeta^- > 0 | \delta_z^2 \zeta^- - V_{zero}^{max} > 0\}. \tag{33}$$

Theorem 2: Under the hypotheses RH1–RH5, GH1–GH5, IH1–IH6, and HH1–HH5 in Appendix A and IFH1–IFH7, with the foot force defined as in (24),

$$\zeta^* = -\frac{V_{zero}(\theta^-)}{1 - \delta_z^2} \tag{34}$$

is an exponentially stable fixed point of (32) if, and only if,

$$0 < \delta_z^2 < 1 \tag{35}$$

$$\frac{\delta_z^2}{1-\delta_z^2} V_{zero}(\theta^-) + V_{zero}^{max} < 0. \tag{36}$$

Proof: $\mathcal{D}$ is non-empty if, and only if, $\delta_z^2 > 0$. If there exists $\zeta^* \in \mathcal{D}$ satisfying $\rho(\zeta^*) = \delta_z^2 \zeta^* - V_{zero}$, then ζ^* is an exponentially stable fixed point if, and only if, $0 < \delta_z^2 < 1$, and in this case, (34) is the value of ζ^*. Finally, (36) is the necessary and sufficient condition for (34) to be in $\mathcal{D}$. ■

Note that this is identical to the result of Westervelt *et al.*[1] if r_f is set to be zero. Using (23), the condition (35) yields that Mv_c^{v-}, the value of the vertical component of the robot's linear momentum, should be negative just before impact, and for stability, $\cos\phi_1 F_f$, the intensity of the vertical component of the foot force, should not exceed $|Mv_c^{v-}|$. More precisely, let $\Upsilon_c(q) = [\Upsilon_c^h(q)\ \Upsilon_c^v(q)]^T$ be the Cartesian coordinates of the center of mass. Then $\Upsilon_c(q)$ is a function of configuration variables only, and the velocity of the center of mass just before the impact is given as follows:

$$v_c^- = \begin{bmatrix} v_c^{h-} \\ \\ v_c^{v-} \end{bmatrix} = \frac{\partial \Upsilon_c(q)}{\partial q}\bigg|_{q=q^-} \dot{q}^-. \tag{37}$$

Then, with the foot force defined in (26), the impact map (23) becomes

$$\begin{aligned} \sigma^+ &= \sigma^- + lM\frac{\partial \Upsilon_c^v}{\partial q}\Phi_{\dot{q}}\sigma^- + \cos\phi_1 r_f \sigma^- && (38)\\ &= (1 + lM\frac{\partial \Upsilon_c^v}{\partial q}\Phi_{\dot{q}} + \cos\phi_1 r_f)\sigma^- && (39)\\ &= \delta_z \sigma^-, && (40) \end{aligned}$$

where $\delta_z < 1$ is necessary for stability.

Differentiating the output $y = h(x)$ twice gives

$$\begin{aligned} \ddot{y} &:= v && (41)\\ &= L_f^2 h(x) + L_g L_f h(x)\Gamma. && (42) \end{aligned}$$

Let v be any control input satisfying controller hypotheses CH2–CH5 in Westervelt *et al.*[1], see Appendix A. Then the zero dynamics manifold for the single support phase is invariant. In this paper, v is defined as

$$v = \frac{1}{\epsilon^2}\nu(y, \epsilon\dot{y}), \tag{43}$$

where ν is the finite settling-time controller by Bhat and Bernstein[19] and $\epsilon > 0$ is a constant for adjusting the settling

time, see Appendix D. The feedback for the full-model (12) is given as follows,

$$\Gamma = (L_g L_f h(x))^{-1}(v(h(x), L_f h(x)) - L_f^2 h(x)). \tag{44}$$

By Theorem 2 in Grizzle *et al.*[13], the full state model is asymptotically stable if, and only if, the reduced Poincaré map (32) has an exponentially stable fixed point. Therefore, the full system is asymptotically stable.

V. PARAMETRIZATION AND OPTIMIZATION OF THE HYBRID ZERO DYNAMICS

As developed in the previous section, controlling the robot is realized by imposing constraints as an output function, which is driven to zero using feedback. Thus, designing an optimal feedback u, that is, a control that creates a stable periodic orbit while meeting a performance objective, is equivalent to designing an optimal output $h(q)$.

The output $y = h(q)$ is selected to have the form

$$y = h(q) = H_0 q - h^d(\theta(q)), \tag{45}$$

where H_0 is a $(N-1) \times N$ constant matrix, $h^d(\theta(q))$ is a desired function for $H_0 q$ to track, and $\theta(q) = cq$ satisfies HH3 so that $[H_0^T \ c^T]^T$ has full rank. The desired function $h^d(\theta(q)) = h^d(s) \circ \theta(q)$ is chosen to be a $(N-1) \times 1$ vector whose elements are Bézier polynomials. Let $b_i(s)$ be Bézier polynomial with order $M \geq 3$

$$b_i(s) := \sum_{k=0}^{M} \alpha_k^i \frac{M!}{k!(M-k)!} s^k (1-s)^{M-k}. \tag{46}$$

Then $h^d(\theta(q)) = [b_i(s), \cdots, b_{N-1}(s)]^T$, with

$$s(\theta(q)) = \frac{\theta(q) - \theta^+}{\theta^- - \theta^+}. \tag{47}$$

Let $\alpha_k = [\alpha_k^1, \cdots, \alpha_k^{N-1}]^T$ where the constants α_k^i are the coefficients of the Bézier polynomials in (46). Let the foot force be defined as in (26). Then (16) and (17) are satisfied when

$$\begin{bmatrix} \alpha_0 \\ \theta^+ \end{bmatrix} = HRH^{-1} \begin{bmatrix} \alpha_M \\ \theta^- \end{bmatrix}, \tag{48}$$

and

$$\alpha_1 = \frac{H_0(\theta^- - \theta^+)(\Delta_{\dot{q}2}\Phi_{\dot{q}}(q^-) + \Delta_{\dot{q}1} r_f)}{Mc(\Delta_{\dot{q}2}\Phi_{\dot{q}}(q^-) + \Delta_{\dot{q}1} r_f)} + \alpha_0. \tag{49}$$

Note that since the foot actuation does not affect the position states, the condition for α_0 to satisfy (16) is identical to the model of unactuated point feet. An optimal control can be found by optimizing the output parameters. The cost function to be optimized is defined as

$$J = \frac{1}{L_s}\left(W_j + W_f\right), \tag{50}$$

where L_s is the step length, W_j is the sum of the work done by the joints, and W_f is the work done by foot actuation.

The total work done by the joints is defined as

$$W_j = \sum_{i=1}^{N-1} \int_{T_s^+}^{T_s^-} |\dot{q}_i \Gamma_i| \, dt, \tag{51}$$

where T_s^+, T_s^- represent the beginning and ending time of a step.

The work done by the impulsive foot action is defined as follows. Let t_I be the impact time and $\tau = E_e^1 \delta F_1 = E_e^1 F_1 \delta(t - t_I)$ from (2) be the effective impulsive torque of the foot. Then the work by the impulsive foot actuation is given by

$$W_f = \int_{t_I^-}^{t_I^+} \tau^T \dot{q}_e \, dt = \int_{t_I^-}^{t_I^+} (E_e^1 F_1 \delta(t - t_I))^T \dot{q}_e \, dt. \tag{52}$$

Due to the impulsive foot actuation, there exists a discontinuous change in the velocity states. Let $\Delta \dot{q}_e = \dot{q}_e^+ - \dot{q}_e^-$ then the velocity states can be written as

$$\dot{q}_e = \Delta \dot{q}_e u(t - t_I) + \dot{\bar{q}}_e, \tag{53}$$

where $u(t)$ is the unit step function. Note that $\dot{\bar{q}}_e$ is continuous and $\Delta \dot{q}_e$ can be obtained from (4) as

$$\Delta \dot{q}_e = (D_e)^{-1} E_e^1 F_1. \tag{54}$$

From (52) and (53), the work done by foot actuation can be obtained as

$$\begin{aligned} W_f &= (E_e^1 F_1)^T \Delta \dot{q}_e \int_{t_I^-}^{t_I^+} \delta(t - t_I) u(t - t_I) \, dt \\ &\quad + (E_e^1 F_1)^T \dot{q}_e^-. \end{aligned} \tag{55}$$

By Hypothesis GH2 in Appendix A, which is the stance leg end acting as a pivot during the single support phase,

$$\frac{\partial \Upsilon_1(q_e)}{\partial q_e} \dot{q}_e^- = (E_e^1)^T \dot{q}_e^- = 0, \tag{56}$$

where $\Upsilon_1(q_e)$ is the Cartesian coordinates of the stance leg end. With (56) and (54), the work by the foot actuation becomes

$$W_f = (E_e^1 F_1)^T (D_e)^{-1} E_e^1 F_1 \int_{t_I^-}^{t_I^+} \delta(t - t_I) u(t - t_I) \, dt. \tag{57}$$

For the work by the foot to be calculated, it is required to determine the value of $\int_{t_I^-}^{t_I^+} \delta(t - t_I) u(t - t_I) \, dt$. Although the integration is not defined at $t = t_I$ in general, in this paper it is taken to be $\int_{t_I^-}^{t_I^+} \delta(t - t_I) u(t - t_I) \, dt = \frac{1}{2}$.

Since the hybrid zero dynamics needs to be achieved during walking, (48) and (49) should be satisfied. Therefore, only $(N-1) \times (M-1)$ coefficients of (46) need to be determined. The detailed constraints for optimization are given in

Westervelt *et al.*[1], which ensure a valid stable walking motion.

IMPULSIVE FOOT CONSTRAINT: An additional constraint on foot actuation is necessary to ensure the applied foot force is unilateral.

IFC1) Foot force, δF_f, is unilateral.

VI. EXAMPLE

This section illustrates the above results on a robot with impulsive foot action. The robot is the 5-link planar bipedal robot[17] with an impulsive actuator added to each foot. For the output function, the order of the Bézier polynomials was set to be $M = 6$. For optimization, the *fmincon* function in MATLAB was used. Table I shows the work done by the joint actuators and the foot actuator when the average walking speed is constrained to be 1 (m/s). The work is normalized by the distance travelled during one step (50). The normalized work done by the robot with foot actuation is less than the robot without foot actuation, which implies that having foot actuation helps to reduce the work required to walk. Table II shows the optimization results with a constrained energy per distance travelled instead of constrained walking speed. The energy constrained is 25 (J/m). With the same amount of energy, the robot with impulsive foot action walks at 0.99 (m/s) whereas the robot without foot action walks at 0.84 (m/s), which also shows the efficiency of impulsive foot action in walking. An animation is available on the web[20]. Table III shows the optimization results with different walking speed. δ_z for the robot with impulsive foot action is larger than for the robot without impulsive foot action, which implies that the convergence rate of the robot with impulsive foot action is slower.

The detailed simulation data of the robot with impulsive foot action are shown in the following figures. The walking speed is set to be 1 (m/s). Fig. 4 is the stick diagram of the robot for one stride. Fig. 5 shows the velocity states of each joint. The open circle and the open square represent the state after foot actuation and before the impact. The foot force on the stance foot is shown in Fig. 6. The stance leg will not slip for a friction coefficient greater than 0.6. The output is plotted in Fig. 7, showing that the controller has indeed driven the output to zero in finite time. Fig. 8 and Fig. 9 are the applied torque at each joint. The torques applied at the stance hip, the swing hip, the stance knee, and the swing knee are represented by u_1, u_2, u_3, and u_4, respectively. Fig. 8 is the plot of torques of the robot without foot actuation and Fig. 9 is the plot of torques of the robot with foot actuation. The robot with foot actuation requires smaller torques are applied during walking. In particular, smaller torques between the torso and two femurs of the robot with foot actuation. Fig. 10 shows the phase portraits of the states. It is clear that the solution converges to a limit cycle.

VII. CONCLUSION

A robot model with impulsive foot actuation was studied. The model was developed from a model with unactuated point feet by Westervelt *et al.*[1] and the work by Kuo[2]. The impulsive actuator at the end of the stance foot was assumed to be active only in the double support phase, which resulted in the single support phase model being identical to the model of the robot with unactuated point feet for the single support phase. However, the double support map depended on the impulsive foot force, which resulted in changes in the zero dynamics. In general, the output function cannot be designed to achieve the hybrid zero dynamics without knowing the foot force a priori. A method to design output functions to achieve the hybrid zero dynamics was given for a class of foot actuation control policies. The stability of the resulting walking motion was shown with a Poincaré map. These results were applied to a 5-link biped robot. The robot with impulsive foot action showed more energy efficient walking than the model without foot action.

APPENDIX

A. Hypotheses

The following hypotheses are based on the hypotheses in Westervelt *et al.*[1] The hypotheses for the robot are:

RH1) The robot consists of N rigid links with revolute joint;

RH2) The robot is planar;

RH3) The robot is bipedal with identical legs connected at hips;

RH4) The joints are actuated;

RH5) The coordinate of the robot consists of $N-1$ relative angles, $q_1, \cdots, q_{N-1}$, and one absolute angle, q_N.

The hypotheses for gait are:

GH1) Walking consists of two alternating phases, single support phase and double support phase;

GH2) The stance feet acts as a pivot during the single support phase;

GH3) The swing leg has neither slipping nor rebounding at impact;

GH4) Successive single support phases are identical with respect to the two legs in steady state;

GH5) Walking is from left to right, so that the swing leg moves from behind the stance leg and touches the ground in front of the stance leg at impact.

The hypotheses for impact are:

IH1) The swing leg has neither rebound nor slipping during impact;

IH2) After impact, the stance leg leaves the ground without any interaction with the ground;

IH3) The impact is instantaneous;

IH4) The reaction force due to the impact can be modelled as an impulse;

IH5) The impulsive force results in discontinuous changes in the velocities while the position states remain continuous;

IH6) The actuators at joints are not impulsive.

Let the output y be $y = h(x)$ then the hypotheses are:

HH1) The output function $h(x)$ being a function of only the configuration coordinates during the single support phase;

HH2) The decoupling matrix $L_g L_f h$ being invertible for an open set $\tilde{\mathcal{Q}} \subset \mathcal{Q}$;

HH3) Existence of $\theta(q)$ such that $[h(q);\ \theta(q)]$ is diffeomorphism;

HH4) h vanishing at least one point.

HH5) Existence of an unique point $q^- \in \tilde{\mathcal{Q}}$ such that $(h(q^-), p_2^v(q^-)) = (0,0), p_2^h(q^-) > 0$ and the rank of $[h^T\ p_2^v]^T$ at q^- equals to N.

The hypotheses for the closed-loop chain of double integrators, $\ddot{y} = v$, are:

CH1) Global invertibility of the decoupling matrix.

CH2) Existence of solutions on $\mathbb{R}^{2N-2}$ and uniqueness;

CH3) Solutions depending continuously on the initial conditions;

CH4) The origin being globally asymptotically stable and the convergence being achieved in finite time;

CH5) The settling time depending continuously on the initial condition.

B. Proof of property 1, 2, 3, and 4

Proof: [Property 1] Let (p_c^h, p_c^v) be the Cartesian coordinates of the center of mass of the robot. Let $\vec{r}_1$ be a vector from the stance foot to the center of mass and let $\vec{r}_3$ be the vector from the stance foot to the swing foot. Let Ψ and ψ be the angle between $\vec{r}_1$ and the ground, and the angle between $\vec{r}_1$ and $\vec{r}_3$, respectively. Let q_N be the absolute angle in the counterclockwise direction, see Fig. 11.

Then $|\vec{r}_1|$ and ψ are independent of q_N and $\Psi = \psi + q_N - q_{N,0}$, where $q_{N,0}$ is a scalar such that the swing leg end touches the ground at $q_N = q_{N,0}$ while the relative angles $q_1, \cdots, q_{N-1}$ are unchanged. Therefore, the coordinates of the center of mass are

$$p_c^h = |\vec{r}_1| \cos(\psi + q_N - q_{N,0}) \tag{58}$$

$$p_c^v = |\vec{r}_1| \sin(\psi + q_N - q_{N,0}). \tag{59}$$

The partial derivatives of (58) and (59) with respect to q_N are given as

$$\frac{\partial p_c^h}{\partial q_N} = -|\vec{r}_1|\sin(\psi + q_N - q_{N,0}) = -p_c^v \tag{60}$$

$$\frac{\partial p_c^v}{\partial q_N} = |\vec{r}_1|\cos(\psi + q_N - q_{N,0}) = p_c^h. \tag{61}$$

The Lagrangian is defined as $L = K - V$, where K is the kinetic energy and V is the potential energy of the robot. Since K does not depend on q_N and $V = Mgp_c^v$ with g being gravitational acceleration and M being total mass,

$$\frac{d}{dt}\frac{\partial L}{\partial \dot{q}_N} = \frac{\partial L}{\partial q_N} = -\frac{\partial V}{\partial q_N} = -Mgp_c^h. \tag{62}$$

Let σ be the angular momentum about the stance foot. Then,

$$\frac{d\sigma}{dt} = (\vec{r}_1 \times \vec{F}_c) \cdot \vec{e}_3, \tag{63}$$

where $\vec{F}_c$ is the force acting on the center of mass. Since $\vec{r}_1 = p_c^h\vec{e}_1 + p_c^v\vec{e}_2$ and $\vec{F}_c = -Mg\vec{e}_2$,

$$\frac{d\sigma}{dt} = -Mgp_c^h. \tag{64}$$

From (62) and (64), we can deduce that $\partial L/\partial \dot{q}_N = \sigma + C_0$, with some constant C_0. Since $\partial L/\partial \dot{q}_N$ and σ are zero if $(\dot{q}_1, \cdots, \dot{q}_N) = 0$, $C_0 = 0$. Therefore

$$\frac{\partial L}{\partial \dot{q}_N} = \sigma. \tag{65}$$

Since $d_N(q)\dot{q} = \partial L/\partial \dot{q}_N$, $d_N(q)\dot{q}$ is the angular momentum of the robot. ■

Proof: [Property 2] Let L and L_e denote the Lagrangians for the single support phase and double support phase, respectively. Define $L = K - V$ and $L_e = K_e - V_e$, where K and K_e are the kinetic energies and V and V_e are the potential energies. By the hypothesis GH2, $L = L_e|_{(p_1^h, p_1^v, \dot{p}_1^h, \dot{p}_1^v) = (c,0,0,0)}$, where c is constant. Since $d_N(q)\dot{q} = \partial L/\partial \dot{q}_N$, $d_N(q^-)\dot{q}^- = \partial L/\partial \dot{q}_N|_{(q,\dot{q}) = (q^-, \dot{q}^-)} = \partial L_e/\partial \dot{q}_N|_{(q, p_1^h, p_1^v, \dot{q}, \dot{p}_1^h, \dot{p}_1^v) = (q^-, c, 0, \dot{q}^-, 0, 0)} = d_{e,N}(q_e^-)\dot{q}_e^-$ ■

Proof: [Property 3] In the given coordinates, the Cartesian coordinates of the stance foot are given by $\Upsilon_1(q_e) = (p_1^h, p_1^v)$. Therefore, $E_N = (\partial \Upsilon_1/\partial q_N)^T = 0$. Thus, from (4), $d_{e,N}(q_e^{1+})\dot{q}_e^{1+} - d_{e,N}(q_e^{1-})\dot{q}_e^{1-} = 0$. ■

Proof: [Property 4] Let $q_c = (q_1, \cdots, q_N, p_c^h, p_c^v)$ be the coordinates of the robot, where p_c^h, p_c^v denote the Cartesian coordinates of the center of mass, see Fig. 11. Then the kinetic energy K_e does not depend on p_c^h, p_c^v and the potential energy is given by $V_e = Mgp_c^v$. Since the force acting on the center of mass is $F_h = 0, F_v = -Mg$,

$$\frac{d}{dt}\frac{\partial L_e}{\partial \dot{p}_c^h} = -\frac{\partial V_e}{\partial p_c^h} = \quad 0 \quad = F_h \tag{66}$$

$$\frac{d}{dt}\frac{\partial L_e}{\partial \dot{p}_c^v} = -\frac{\partial V_e}{\partial p_c^v} = -Mg = F_v. \tag{67}$$

Therefore, $\frac{\partial L_e}{\partial \dot{p}_c^h}, \frac{\partial L_e}{\partial \dot{p}_c^v}$ are the linear momentum. In the coordinates q_c, let $\Upsilon_1(q_c)$ be the Cartesian coordinates of the stance foot. Then, $\vec{P}_c^+ - \vec{P}_c^- = \mathcal{T} F_f$. ■

C. Proof of theorem 1

Proof: (Necessity) Assume $\forall z^- = (\theta^-, \sigma^-) \in S \cap Z$, there exists $F_f \in \mathbb{R}^+ \cup \{0\}$ such that $L_f h \circ \Delta(z^-, F_f) = 0$. Let $z_1^- = (\hat{\theta}^-, \sigma_1^-) \in S \cap Z$ and $F_f^1 \neq 0$ be a point in $S \cap Z$ and a foot force satisfying $L_f h \circ \Delta(z_1^-, F_f^1) = 0$.

$$\begin{aligned} L_f h \circ \Delta(\hat{z}^-, \hat{F}_f) = 0 \iff & \frac{\partial h}{\partial q}(q^+)\dot{q}^+ = 0 \\ \iff & w_1 \hat{F}_f + w_2 \hat{\sigma}^- \in \mathcal{N}\left(\frac{\partial h}{\partial q}(q^+)\right) \qquad (68) \\ L_f h \circ \Delta(z_1^-, F_f^1) = 0 \iff & \frac{\partial h}{\partial q}(q^+)\dot{q}^+ = 0 \\ \iff & w_1 F_f^1 + w_2 \sigma_1^- \in \mathcal{N}\left(\frac{\partial h}{\partial q}(q^+)\right), \qquad (69) \end{aligned}$$

where w_1, w_2 are $N \times 1$ vectors defined in (20) and $\mathcal{N}\left(\frac{\partial h}{\partial q}(q^+)\right)$ is the null space of $\frac{\partial h}{\partial q}(q^+)$. Since $\hat{\sigma}^- \neq 0$, there exists $r \in \mathbb{R}$ such that $\sigma_1^- = r\hat{\sigma}^-$. From (68) and (69),

$$\begin{aligned} & r w_1 \hat{F}_f + r w_2 \hat{\sigma}^- - (w_1 F_f^1 + w_2 \sigma_1^-) \\ = \quad & w_1 (r\hat{F}_f - F_f^1) \in \mathcal{N}\left(\frac{\partial h}{\partial q}(q^+)\right). \qquad (70) \end{aligned}$$

Since (70) is true if, and only if, either $w_1 \in \mathcal{N}\left(\frac{\partial h}{\partial q}(q^+)\right)$ or $r\hat{F}_f - F_f^1 = 0$, these cases are now studied separately.

Case 1. If $w_1 \notin \mathcal{N}\left(\frac{\partial h}{\partial q}(q^+)\right)$ and $r\hat{F}_f = F_f^1$, then, because $\sigma_1^- = r\hat{\sigma}^-$, $r = \frac{\sigma_1^-}{\hat{\sigma}^-}$. Therefore,

$$F_f^1 = \frac{\hat{F}_f}{\hat{\sigma}^-}\sigma_1^-. \qquad (71)$$

Case 2. If $w_1 \in \mathcal{N}\left(\frac{\partial h}{\partial q}(q^+)\right)$, then (68) implies $w_2 \in \mathcal{N}\left(\frac{\partial h}{\partial q}(q^+)\right)$ since $\hat{\sigma}^- \neq 0$. Since $w_1 \neq 0$ by hypothesis, and the

null space is 1 dimensional, there exists $\lambda \in \mathbb{R}$ such that $w_2 = \lambda w_1$. From the impact map (10),

$$w_2 - \lambda w_1 = 0 \iff \begin{bmatrix} R & 0 \end{bmatrix} \Pi \left(\begin{bmatrix} D_e \begin{bmatrix} \Phi_{\dot{q}} \\ 0 \end{bmatrix} \\ 0 \end{bmatrix} - \lambda \begin{bmatrix} E_e^1 \mathcal{T} \\ 0 \end{bmatrix} \right) = 0 \tag{72}$$

$$\iff \Pi \left(\begin{bmatrix} D_e \begin{bmatrix} \Phi_{\dot{q}} \\ 0 \end{bmatrix} \\ 0 \end{bmatrix} - \lambda \begin{bmatrix} E_e^1 \mathcal{T} \\ 0 \end{bmatrix} \right) \in \mathcal{N} \left(\begin{bmatrix} R & 0 \end{bmatrix} \right) \tag{73}$$

$$\iff \left(\begin{bmatrix} D_e \begin{bmatrix} \Phi_{\dot{q}} \\ 0 \end{bmatrix} \\ 0 \end{bmatrix} - \lambda \begin{bmatrix} E_e^1 \mathcal{T} \\ 0 \end{bmatrix} \right) = \Pi^{-1} \begin{bmatrix} 0_{N\times 1} \\ \xi_1 \\ \xi_2 \\ \xi_3 \\ \xi_4 \end{bmatrix}, \tag{74}$$

where $\xi_1, \xi_2, \xi_3, \xi_4$ are scalars and Π is a $(N+4) \times (N+4)$ matrix defined in (9). From the last two rows of (74),

$$\begin{bmatrix} (E_e^2)^T & 0 \end{bmatrix} \begin{bmatrix} 0_{N\times 1} \\ \xi_1 \\ \xi_2 \\ \xi_3 \\ \xi_4 \end{bmatrix} = (E_e^2)^T \begin{bmatrix} 0_{N\times 1} \\ \xi_1 \\ \xi_2 \end{bmatrix} = 0 \tag{75}$$

$$\iff (E_{e,2}^2)^T \begin{bmatrix} \xi_1 \\ \xi_2 \end{bmatrix} = 0, \tag{76}$$

where $(E_{e,2}^2)^T$ is last two columns of $(E_e^2)^T$. Since $(E_{e,2}^2)^T$ has full rank, $\xi_1 = \xi_2 = 0$. Therefore, from (74),

$$D_e \begin{bmatrix} \Phi_{\dot{q}} \\ 0 \end{bmatrix} - \lambda E_e^1 \mathcal{T} = -E_e^2 \begin{bmatrix} \xi_3 \\ \xi_4 \end{bmatrix}. \tag{77}$$

(Sufficiency)

Case 1. Since $w_1 \hat{F}_f + w_2 \hat{\sigma}^- \in \mathcal{N}\left(\frac{\partial h}{\partial q}(q^+)\right)$ and $\hat{\sigma}^- \neq 0$, $(w_1 \frac{\hat{F}_f}{\hat{\sigma}^-} + w_2) \in \mathcal{N}\left(\frac{\partial h}{\partial q}(q^+)\right)$. For $F_f = \frac{\hat{F}_f}{\hat{\sigma}^-}\sigma^-$, the impact map (20) becomes

$$\dot{q}^+ = w_1 F_f + w_2 \sigma^- \tag{78}$$

$$= w_1 \frac{\hat{F}_f}{\hat{\sigma}^-}\sigma^- + w_2 \sigma^- \tag{79}$$

$$= \sigma^- (w_1 \frac{\hat{F}_f}{\hat{\sigma}^-} + w_2) \in \mathcal{N}\left(\frac{\partial h}{\partial q}(q^+)\right). \tag{80}$$

Case 2. Let $\lambda \in \mathbb{R}$ and $\hat{v} \in \mathbb{R}^2$ such that

$$D_e \begin{bmatrix} \Phi_{\dot{q}} \\ 0 \end{bmatrix} - \lambda E_e^1 \mathcal{T} = -E_e^2 \hat{v}. \tag{81}$$

Multiplying (81) by $\hat{\sigma}^-$ yields,

$$D_e\dot{q}_e^- - \lambda\hat{\sigma}^- E_e^1\mathcal{T} = -E_e^2\hat{v}\hat{\sigma}^-. \tag{82}$$

From the impact map (20) and (82),

$$\begin{aligned}
\dot{q}^+ &= w_1\hat{F}_f + w_2\hat{\sigma}^- && (83)\\
&= \begin{bmatrix} R & 0 \end{bmatrix}\Pi\begin{bmatrix} -E_e^2\hat{v}\hat{\sigma}^- \\ 0 \end{bmatrix} + \begin{bmatrix} R & 0 \end{bmatrix}\Pi\begin{bmatrix} (\hat{F}_f + \lambda\hat{\sigma}^-)E_e^1\mathcal{T} \\ 0 \end{bmatrix} && (84)\\
&= (\hat{F}_f + \lambda\hat{\sigma}^-)\Pi\begin{bmatrix} E_e^1\mathcal{T} \\ 0 \end{bmatrix} && (85)\\
&= (\hat{F}_f + \lambda\hat{\sigma}^-)w_1, && (86)
\end{aligned}$$

since

$$\begin{bmatrix} R & 0 \end{bmatrix}\Pi\begin{bmatrix} -E_e^2\hat{v}\hat{\sigma}^- \\ 0 \end{bmatrix} = 0. \tag{87}$$

$(\hat{F}_f + \lambda\hat{\sigma}^-) \neq 0$ in (86) since $\dot{q}^+ \neq 0$. Therefore, $w_1\hat{F}_f + w_2\hat{\sigma}^- = (\hat{F}_f + \lambda\hat{\sigma}^-)w_1$ implies $w_1 \in \mathcal{N}\left(\frac{\partial h}{\partial q}(q^+)\right)$, which also implies $w_2 \in \mathcal{N}\left(\frac{\partial h}{\partial q}(q^+)\right)$. Therefore, $\forall z^- \in S \cap Z$ and $F_f \in \mathbb{R} \cup \{0\}$, $w_1F_f + w_2\sigma^- \in \mathcal{N}\left(\frac{\partial h}{\partial q}(q^+)\right)$.

■

D. Finite settling time controller for double integrators

The following controller is the finite-settling time controller for a double integrator developed by Bhat and Bernstein [19]. Consider the double integrator

$$\begin{aligned}
\dot{y}_1 &= y_2 \\
\dot{y}_2 &= \nu. && (88)
\end{aligned}$$

The double integrator (88) is globally finite-time stabilizable with continuous feedback control

$$\nu = -\text{sign}(y_2)|y_2|^\alpha - \text{sign}(\phi_\alpha(y_1, y_2))|\phi_\alpha(y_1, y_2)|^{\frac{\alpha}{2-\alpha}}, \tag{89}$$

where $\phi_\alpha(y_1, y_2) := y_1 + \frac{1}{2-\alpha}\text{sign}(y_2)|y_2|^{2-\alpha}$ and $0 < \alpha < 1$. The settling time, T_{set}, depends continuously on the initial condition.

ACKNOWLEDGMENTS

This work was supported by NSF grant ECS-0322395. The authors thank Christine Chevallereau of the CNRS for helpful comment on impact maps and conservation of angular momentum.

REFERENCES

1. E. R. Westervelt, J. W. Grizzle, and D. E. Koditschek, "Hybrid zero dynamics of planar biped walkers," *IEEE Trans. Automatic Control*, vol. 48, no. 1, pp. 42–56, 2003.
2. A. D. Kuo, "Enegetics of actively powered locomotion using the simplest walking model," *J. of Biomechanical Engineering*, vol. 124, pp. 113–120, February 2002.
3. G. A. Cavagna and R. Margaria, "Mechanics of walking," *J. of Applied Physiology*, vol. 21, no. 1, pp. 271–278, 1966.
4. T. McGeer, "Passive dynamic walking," *Int. J. of Robotics Research*, vol. 9, no. 2, pp. 62–82, 1990.
5. R. Q. van der Linde, "Active leg compliance for passive walking," in *Proc. Int. Conf. Robotics and Automation*, Leuven, Belgium, May 1998, pp. 2339–2344.
6. K. Y. Yi, "Walking of a biped robot with passive ankle joints," in *Proc. Int. Conf. Control Application*, Kohala Coast-Island of Hawaii, Hawaii, USA, August 1999, pp. 484–489.
7. F. Asano, M. Yamakita, N. Kamamichi, and Z.-W. Luo, "A novel gait generation for biped walking robots based on mechanical energy constraint," in *Proc. IEEE/RSJ Int. Conf. Intelligent Robots and Systems*, Lausanne, Switzerland, October 2002, pp. 2637–2644.
8. K. Hirai, M. Hirose, Y. Haikawa, and T. Takenaka, "The development of honda humanoid robot," in *Proc. Int. Conf. Robotics and Automation*, Leuven, Belgium, May 1998, pp. 1321–1326.
9. H.-O. Lim, S. A. Setiawan, and A. Takanishi, "Balance and impedance control for biped humanoid robot locomotion," in *Proc. IEEE/RSJ Int. Conf. Intelligent Robots and Systems*, Maui, Hawaii, October 2001, pp. 494–499.
10. C.-L. Shih, "The dynamics and control of a biped walking robot with seven degrees of freedom," *J. of Dynamic Systems, Measurement, and Control*, vol. 118, pp. 683–690, December 1996.
11. A. Sano and J. Furusho, "Realization of natural dynamic walking using the angular momentum information," in *Proc. IEEE Int. Conf. Robotica and Automation*, Cincinnati, OH, May 1990, pp. 1476–1481.
12. T. Takahashi and A. Kawamura, "Posture control using foot toe and sole for biped walking robot "ken"," in *Int. Workshop on Advanced Motion Control*, Maribor, Slovenia, 2002, pp. 437–442.

13. J. W. Grizzle, G. Abba, and F. Plestan, "Asymptotically stable walking for biped robots: Analysis via systems with impulse effects," *IEEE Trans. Automatic Control*, vol. 46, no. 1, pp. 51–64, 2001.

14. E. R. Westervelt, G. Buche, and J. W. Grizzle, "Inducing dynamically stable walking in an underactuated prototype planar biped," in *IEEE 2004 Int. Conf. on Robotics and Automation*, October 2003, to appear; see http://www.mecheng.ohio-state.edu/~westerve for a pre-print.

15. E. Westervelt, G. Buche, and J. Grizzle, "Experimental validation of a framework for the design of controllers that induce stable walking in planar bipeds," *The Int. J. of Robotics Research*, to appear; see http://www.mecheng.ohio-state.edu/~westerve for a pre-print.

16. M. Hardt, K. Kreutz-Delgado, and J. W. Helton, "Optimal biped walking with a complete dynamical model," in *Proc. 38th IEEE CDC*, Phoenix, Arizona, USA, December 1999, pp. 2999–3004.

17. C. Chevallereau, G. Abba, Y. Aoustin, F. P. andE. R. Westervelt, C. C. de Wit, and J. W. Grizzle, "Rabbit: A testbed for advanced control theory," *IEEE Control Systems Magazine*, vol. 23, no. 5, pp. 57–79, October 2003.

18. H. Ye, A. N. Michel, and L. Hou, "Stability theory for hybrid dynamical systems," *IEEE Trans. Automatic Control*, vol. 43, no. 4, pp. 461–474, April 1998.

19. S. P. Bhat and D. S. Bernstein, "Continuous finite-time stabilization of the translational and rotational double integrators," *IEEE Trans. Automatic Control*, vol. 43, no. 5, pp. 678–682, May 1998.

20. [Online]. Available: http://www.eecs.umich.edu/~grizzle/ImpulsiveFoot

LIST OF FIGURES

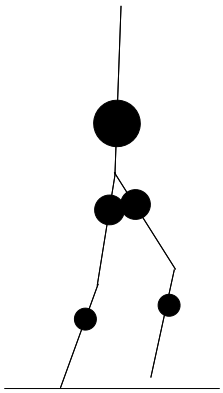

Fig. 1. Typical planar bipedal robot model

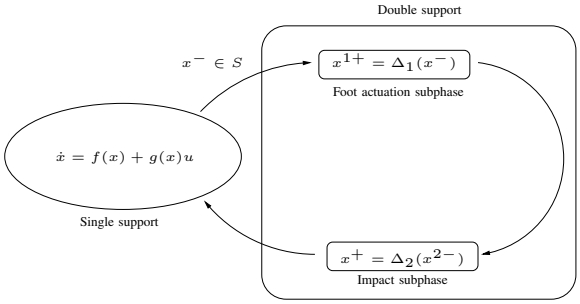

Fig. 2. Phase diagram for the system, which combines the point foot model of Westervelt *et al.* [1] with the impulsive foot action of Kuo [2].

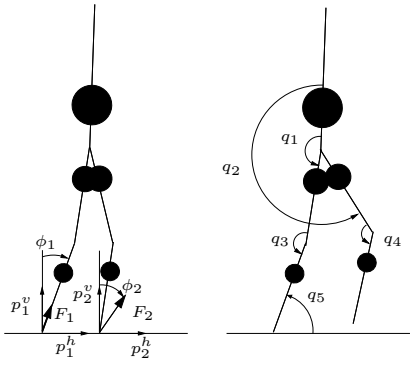

Fig. 3. 5-link robot with impulsive feet during the double support phase and the single support phase. F_1 and F_2 represent the impulsive foot force and the impulsive reaction force due to impacts, respectively.

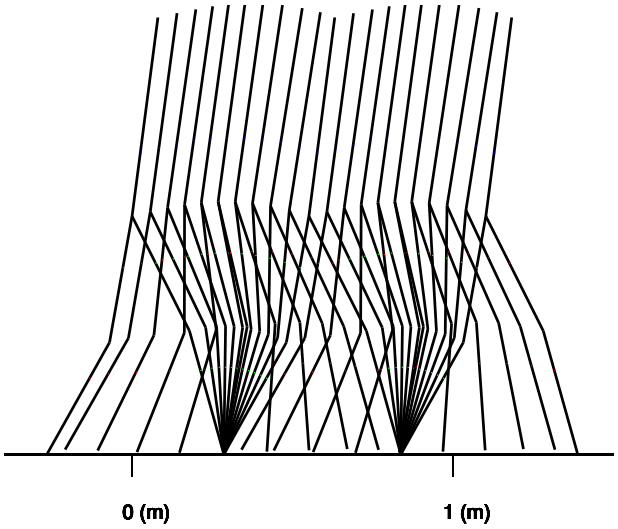

Fig. 4. Stick diagram of the robot for one stride.

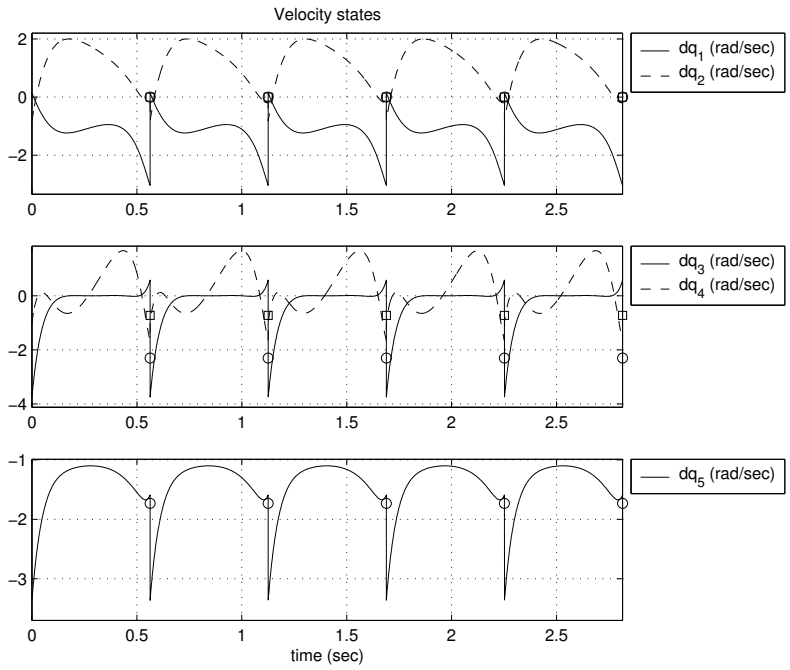

Fig. 5. Velocity states of the robot on the HZD. The walking speed is set to be 1 (m/s). The open circle and square represent the states of the stance leg and the swing leg after the foot force, respectively.

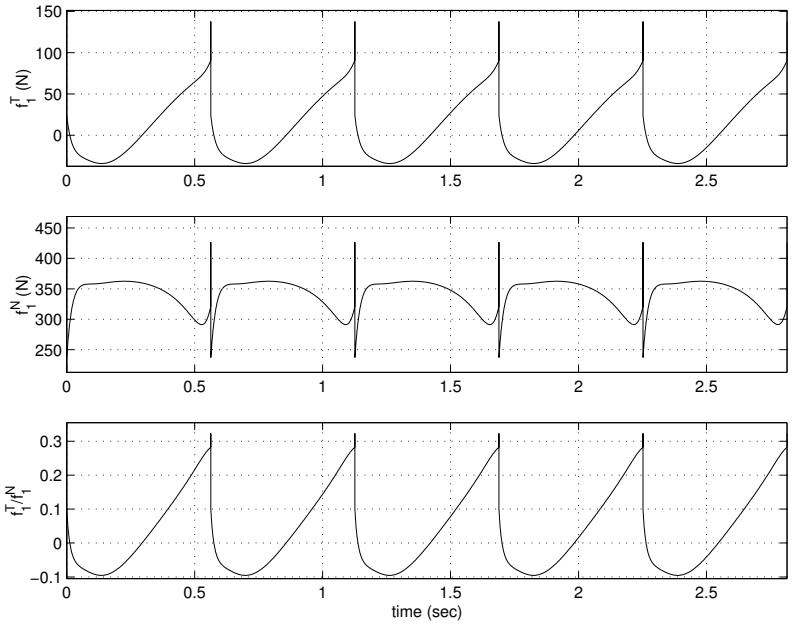

Fig. 6. Foot force at the stance foot on the HZD. The walking speed is set to be 1 (m/s). f_1^T and f_1^N represent the tangential component of the force and the normal component of the force, respectively.

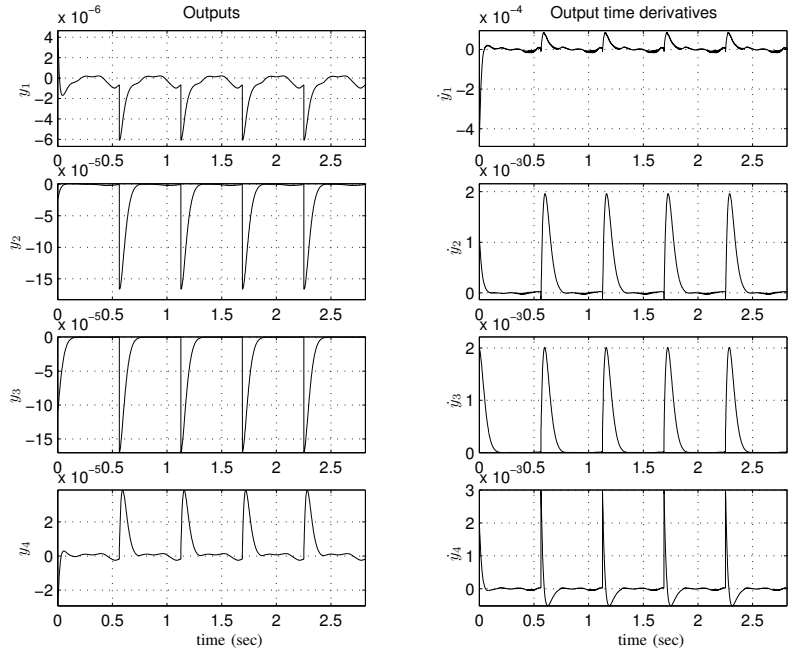

Fig. 7. Output function when the walking speed is set to be 1 (m/s) and the robot is initialized off of the HZD.

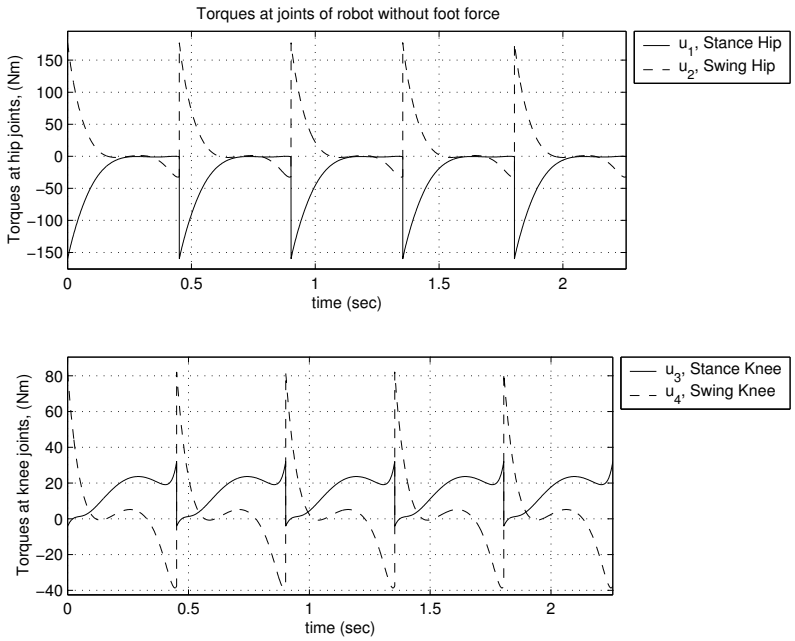

Fig. 8. Torques of the robot without foot actuation on the HZD. The walking speed is set to be 1 (m/s). Dashed lines are torques of the swing leg joints and solid lines are torques of the stance leg joints.

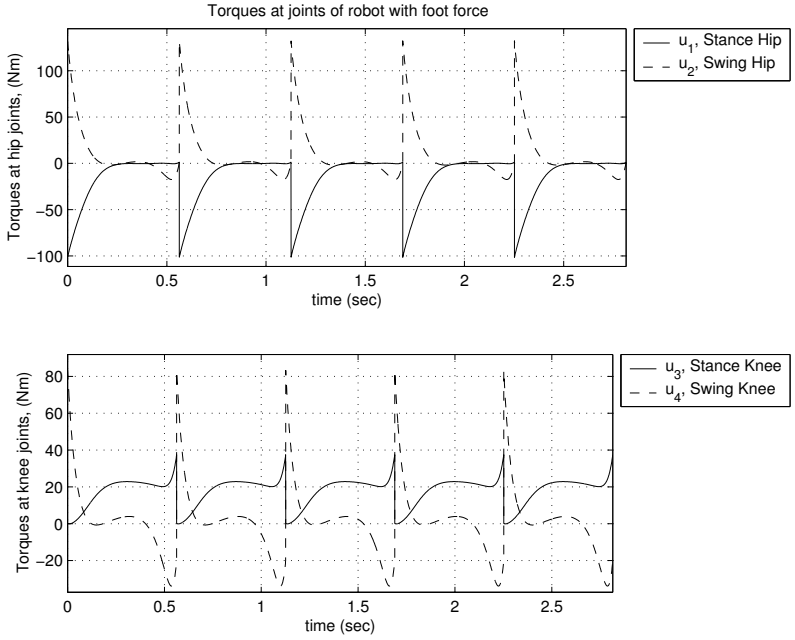

Fig. 9. Torques of the robot with foot actuation on the HZD. The walking speed is set to be 1 (m/s). Dashed lines are torques of the swing leg joints and solid lines are torques of the stance leg joints.

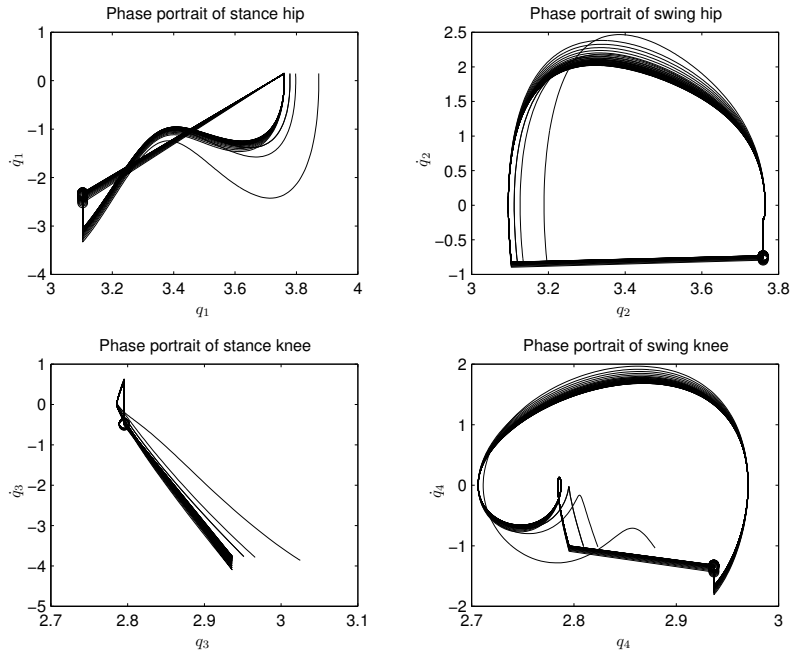

Fig. 10. Phase portraits when the robot is initialized off of the HZD.

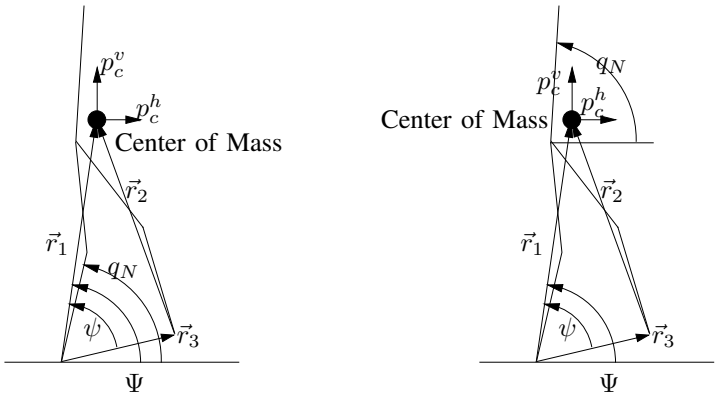

(a) (b)

Fig. 11. Coordinates convention. (a) shows the Cartesian coordinates of the center of mass and one convenient choice for q_N. (b) is an alternative choice for q_N. Any angle referenced to the world frame and measured in the counterclockwise direction is allowed for q_N.

LIST OF TABLES

$F_f(N)$	$W_{total}(J/m)$	$W_j(J)$	$W_f(J)$	L_s(m)
0	34.29	15.47	0	0.45
11.95	25.61	11.85	2.56	0.56

TABLE I

WORK DONE BY THE JOINTS AND THE FOOT PER DISTANCE TRAVELLED. F_f, L_s ARE THE FOOT FORCE AND STEP LENGTH, W_{total} IS TOTAL WORK PER DISTANCE TRAVELLED, W_j, AND W_f ARE WORK BY JOINTS AND WORK BY FOOT, RESPECTIVELY, WHEN THE WALKING SPEED IS 1 M/S.

Cost (J/m)	With Foot Force					Without Foot Force				
	Speed (m/s)	δ_z $-$	$V_{zero}(\theta^-)$ $(kgm^2/s)^2$	V_{zero}^{max} $(kgm^2/s)^2$	Step Length (m)	Speed (m/s)	δ_z $-$	$V_{zero}(\theta^-)$ $(kgm^2/s)^2$	V_{zero}^{max} $(kgm^2/s)^2$	Step Length (m)
25	0.99	0.92	-133.13	404.85	0.549	0.84	0.87	-145.03	216.11	0.430

TABLE II

OPTIMIZATION RESULTS WITH CONSTRAINED REQUIRED ENERGY PER DISTANCE TRAVELLED.

Speed (m/s)	With Foot Force					Without Foot Force				
	Cost (J/m)	δ_z $-$	$V_{zero}(\theta^-)$ $(kgm^2/s)^2$	V_{zero}^{max} $(kgm^2/s)^2$	Step Length (m)	Cost (J/m)	δ_z $-$	$V_{zero}(\theta^-)$ $(kgm^2/s)^2$	V_{zero}^{max} $(kgm^2/s)^2$	Step Length (m)
0.8	18.01	0.937	-76.77	360.81	0.504	23.58	0.858	-156.31	232.99	0.445
0.9	21.61	0.922	-114.41	394.13	0.536	28.49	0.869	-160.11	210.28	0.431
1.0	25.61	0.918	-140.06	426.79	0.563	34.29	0.857	-207.67	217.23	0.451
1.1	29.99	0.915	-167.13	449.12	0.583	40.22	0.848	-255.02	218.28	0.467
1.2	35.20	0.912	-195.74	461.42	0.597	47.83	0.863	-252.06	188.64	0.445

TABLE III

OPTIMIZATION RESULTS WITH CONSTRAINED WALKING SPEED.